Numerical investigation of enhanced thermal performance in phase change materials (PCMs) via nanoparticles across diverse regenerator configurations

Maryam El Fiti[1*], *Mustapha* Salihi[1], *Yasser* Harmen[1], *Ahmed* Chebak[1], and *Younes* Chhiti[1,2]

[1] Green Tech Institute (GTI), Mohammed VI Polytechnic University, Ben Guerir, Morocco
[2] École Nationale Supérieure de Chimie, Ibn Tofail University, Kenitra, Morocco

Abstract. This study investigates the use of CuO-enhanced Paraffin wax (RT-55) in a horizontal co-axial regenerator, addressing the challenge of low thermal conductivity in Phase Change Materials (PCM). The focus is primarily on examining the influence of CuO nanoparticles on the thermal and energetic performance of the regenerator. The research begins by exploring the impact of CuO volume fraction on both the total melting time and energy density. Subsequently, the study incorporates the addition of 3 wt.% of nanoparticles to diverse regenerator configurations, including non-uniform longitudinal fins, eccentricity, and combined fins with eccentricity. The objectives are twofold: firstly, to evaluate the effect of nanoparticles on power densities across various geometries; secondly, to assess the implications of natural convection within each configuration upon nanoparticles addition. The results demonstrate that while the nanoparticles enhance the power density of the system, they concurrently modify the storage capacity of the Latent Thermal Energy Storage System (LTES). Furthermore, the impact of nanoparticles varies depending on the regenerator's configuration, owing to the influence of natural convection. Therefore, it was demonstrated that in the eccentric case, which experiences the highest impact of natural convection, the total melting time is increased by 2% when nanoparticles are added. Conversely, the finned and combined cases show a 4% and 8% reduction in the melting time with the addition of the same amount of CuO nanoparticles.

Keywords: Phase Change Material (PCM), non-uniform fins, regenerator, eccentricity, nanoparticles, combined techniques.

1 Introduction

In recent years, the pursuit of efficient energy utilization has promoted the development of innovative thermal energy storage systems, among which Latent Thermal Energy Storage

* Corresponding author: maryam.elfiti@um6p.ma

(LTES) has garnered significant attention, due to their high energy density and their ability to store and release energy within constant temperature range. One of the primary challenges associated with LTES is the low thermal conductivity of PCM, leading to low power density. To overcome this challenge, many techniques have been proposed in the literature [1]. These techniques range from the incorporation of fins [1–3], eccentricity [4–6], and triplex heat exchangers [7–9], to the utilization of metal foams [10–13] and high conductive nanoparticles [14]. Among these techniques, the integration of nanoparticles has emerged as a promising approach to enhance the thermal performance of LTES systems. Nonetheless, the introduction of nanoparticles introduces a nuanced interaction between enhanced power density and the consequential alterations in energy storage capacity and cost implications, complicated further by the regenerator's specific configuration.

Earlier studies have focused on combining nanoparticles with other thermal enhancement techniques. Zhang et al. [15] suggested combining novel branch-structured fins with Al_2O_3 nanoparticles to improve solidification performance in a triple-tube heat exchanger (TTHX). The numerical study demonstrated that the integration of fins and nanoparticles notably decreased solidification time. Nevertheless, the utilization of metal fins led to higher power densities in comparison to the use of nanoparticles. Similarly, Mahdi and Nsofor [16] conducted a numerical study on the integration of nanoparticles, fins, and PCM within a TTHX to assess its performance during the melting process. The study explored the effects of different fin's dimensions and nanoparticles volumes. Their findings suggested that the combination of fins and nanoparticles with PCM outperformed the pure PCM, fin-PCM, and Nano NEPCM. Sheikholeslami [17] numerically investigated a novel honeycomb configuration filled with a mixture of paraffin and Al_2O_3 nanoparticles, to enhance the charging rate of the LTESS. They analysed the effect of the honeycomb structure material and holes configurations on the melting performance, while they kept the NEPCM volume constant. It was found that the incorporation of Al_2O_3 nanoparticles into paraffin within the novel honeycomb-shaped heat storage system led to faster charging and improved thermal conditions. While several studies have explored the impact of adding nanoparticles alone or in combination with other enhancement techniques to improve the thermal performance of the system, none of them have assessed their influence on different regenerator configurations. This lack of understanding raises the question of whether the use of nanoparticles is universally beneficial, regardless of the specific configuration. In this regard, this study aims to investigate the intricate relationship between CuO nanoparticles, regenerator configuration, and the thermal behaviour of the system, thereby discerning the effects of these elements on the overall performance of LTES. Therefore, the impact of nanoparticles on different regenerator's configurations is still unknown. Notably, understanding the impact of nanoparticles on diverse designs is crucial in determining the optimal enhancement techniques to achieve the highest thermal performance.

2 Numerical study

2.1 Problem statement

Fig. 1 (a) illustrates the 2-D schematic of the physical domain consisting of a horizontal co-axial regenerator.

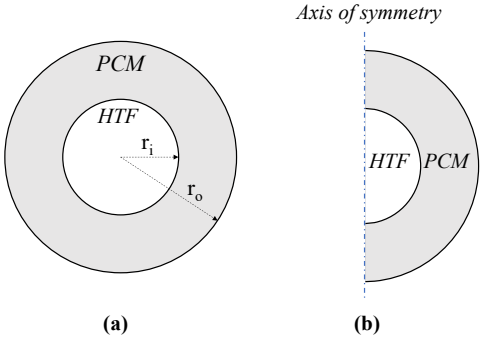

Fig. 1. 2-D schematic of the LTESS, (a) cross section of the physical domain, (b) computational domain.

The PCM fills the annular space between the inner tube and the adiabatic shell. These tubes, made of stainless steel and plexiglass, have diameters of 20 mm and 40 mm, respectively. Paraffin (RT-55) is selected as PCM due to its availability, cost-effectiveness, stability, and the absence of supercooling effect, CuO nanoparticles are chosen for their high thermal conductivity and low cost compared to other nanoparticle's types.
The inner tube is maintained at a constant temperature of 339 K. The initial temperature of the system is set to 323 K. Considering the symmetrical behaviour of the PCM melting inside the regenerator, only the half of the regenerator was simulated. The computational domain is depicted in Fig. 1 (b). Table I presents the thermophysical properties of the materials used in the present study.

Table 1. Thermophysical properties of the PCM (RT-55) and CuO nanoparticles.

	Paraffin (RT-55)	**CuO**
Density (Kg/m3)	Liquid: 880 Solid: 770	6510
Thermal conductivity (W/m.K)	0.2069	18
Specific heat (J/Kg.K)	2011	540
Latent heat (KJ/Kg)	162.77	-
Phase change temperature (K)	325	-

Initially, the simulation included the reference case with various CuO volume fractions to investigate their effects on the total melting time (TMT) and the stored energy. The studied volume fractions were 1 wt.%, 3 wt.%, 5 wt.%, 7 wt.%, and 9 wt.%. Subsequently, 3 wt.% of CuO nanoparticles were introduced into three different configurations employing various heat intensification techniques: the non-uniform longitudinal fin, the eccentricity, and the combined fins and eccentricity. The aim was to analyse how the identical volume fraction of nanoparticles influenced diverse designs and determine whether the enhancements exhibited similar improvements. Fig. 2 illustrates the methodology adopted for this study.

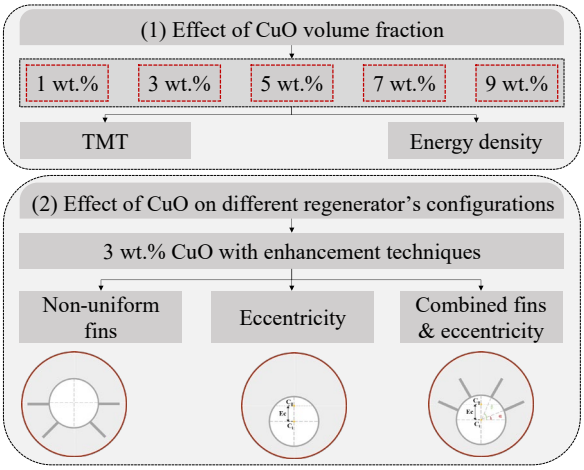

Fig. 2. Workflow of the study.

2.2 Governing equations

The numerical simulation of the PCM melting inside the regenerator considered the following assumptions: (1) The melting behaviour of PCM is axisymmetric; (2) the flow is laminar and unsteady; (3) the thermophysical properties of the HTF and PCM are constant with respect to temperature; (4) the shell wall is assumed adiabatic; (5) the Boussinesq approximation holds, assuming that the density variation is accounted for solely in the buoyancy term. According to this approximation, the density is defined as bellow:

$$\rho = \frac{\rho_{liq}}{\beta(T - T_m) + 1} \tag{1}$$

Where ρ_{liq} is the liquid PCM density, T_m is the PCM phase change temperature, and β is the thermal expansion coefficient.

To numerically solve the PCM melting inside the regenerator, the enthalpy-porosity approach was utilized [18]. The conservation equations of continuity, momentum and energy are defined as follows:

$$\frac{\partial v_i}{\partial x_i} = 0 \tag{2}$$

$$\rho \frac{\partial v_i}{\partial t} + \rho \frac{\partial v_i v_j}{\partial x_j} = \mu \frac{\partial^2 v_i}{\partial^2 v_j^2} - \frac{\partial p}{\partial x_i} + S_B + S_i \tag{3}$$

$$\rho \frac{\partial h}{\partial t} + \rho \frac{\partial v_i h}{\partial x_j} = \frac{\partial}{\partial x_i} k \frac{\partial T}{\partial x_i} \tag{4}$$

Where ρ denotes the density, v represents the velocity, p the pressure, μ is the dynamic viscosity, k defines the thermal conductivity, T the temperature, and h denotes the enthalpy. S_i and S_B represent the momentum and the buoyancy source terms, respectively, and are defined as:

$$S_i = A \frac{1 - \alpha}{LF^3 + \varepsilon} v_i \tag{5}$$

$$S_B = \rho\beta(T - T_m)g \tag{6}$$

Where ε represents a small number implemented to prevent division by zero when LF equals zero, and A denotes the mushy zone constant, with a suggested value from the literature set at 10^5 [19].

The inclusion of the following equations allows for the measurement of the liquid fraction and enthalpy.

$$H = \begin{cases} \int_{T_{ref}}^{T} C_{p,s} dT\,, & T < T_{sol} \\ \int_{T_{ref}}^{T_{sol}} C_{p,s}\, dT + LF\Delta h, & T_{sol} < T < T_{liq} \\ \int_{T_{ref}}^{T_{sol}} C_{p,s}\, dT + L_{PCM} + \int_{T_{liq}}^{T} C_{p,l}\, dT\,, T > T_{liq} \end{cases} \quad (7)$$

$$LF = \frac{H}{L_{PCM}} = \begin{cases} 0, & T < T_{sol} \\ 1, & T > T_{liq} \\ \dfrac{T - T_{sol}}{T_{liq} - T_{sol}}, & T_{sol} < T < T_{liq} \end{cases} \quad (8)$$

Where $C_{p,s}$ and $C_{p,l}$ denotes the PCM specific heat capacity at the solid and liquid states, respectively. while T_{ref} refers to the reference temperature. L_{PCM} represents latent heat of the PCM, T_{liq} and T_{sol} are the melting and solidification temperatures, respectively. The thermophysical properties of NEPCM are obtained using the following equations [20,21]:

$$\rho_{NEPCM} = \alpha\rho_{CuO} + (1 - \alpha)\rho_{PCM} \quad (9)$$

$$Cp_{NEPCM} = \frac{\alpha\rho_{CuO}Cp_{,CuO} + (1 - \alpha)\rho_{PCM}Cp_{,PCM}}{\rho_{NEPCM}} \quad (10)$$

$$\mu_{NEPCM} = \mu_{PCM}(0.9197e^{22.8539\alpha}) \quad (11)$$

$$L_{NEPCM} = \frac{(1 - \alpha)\rho_{PCM}L_{PCM}}{\rho_{NEPCM}} \quad (12)$$

$$K_{NEPCM} = \frac{K_{CuO} + 2K_{PCM} - 2\alpha(k_{PCM} - K_{CuO})}{K_{CuO} + 2 + \alpha(k_{PCM} - K_{CuO})}K_{PCM} \quad (13)$$

Where α describes the nanoparticles volume fraction.

2.3 Computational methodology

The computational study is carried out using the finite volume method with the commercial software Ansys Fluent. V23 R2. The pressure-based solver is adopted to solve the Navier-Stokes and energy equations, and the COUPLED algorithm is used to solve the pressure-velocity coupling. The second-order upwind scheme was utilized to discretize the energy and momentum equations, while the PRESTO method was applied for pressure discretization. A time step of 0.1 s and a mesh size of 49,019 cells were adopted, based on the findings of the previous study [1]. According to the same study, the numerical model was validated against the experimental findings of Dhaidan et al. [22], indicating a strong correlation between the numerical model and the experimental data. it is worth mentioning that the connection between the liquid and solid phases does not account for the displacement of the nanoparticles. The model assumes a uniform dispersion of the CuO nanoparticles within the regenerator during the phase change process.

3 Results and discussion

3.1 Effect of nanoparticles volume fraction

To explore the influence of the CuO nanoparticles on the thermal performance behaviour of the regenerator, six different distinct cases were simulated and compared, including the reference case without any enhancement technique, along with varying volume fractions of CuO nanoparticles: 1 wt.%, 3 wt.%, 5 wt.%, 7 wt.%, and 9 wt.%. The results are presented in the form of mass fraction evolution and stored energy with respect to time. Fig. 3 illustrates the temporal evolution of melting fraction corresponding to the different cases. As shown in the figure, four distinct stages can be observed.

Initially, the curves overlap. In this first stage, the melting rate is at its peak, primarily due to the melting of the first thin layer in direct contact with the inner tube, without any PCM layer impeding the heat transfer, and the impact of nanoparticles is negligible. Subsequently, between 50 s and 400 s, the impact of nanoparticles becomes noticeable, given the predominance of solid PCM and, thus, conduction as the main heat transfer mechanism. Which leads to emphasizing higher melting fractions for cases with elevated CuO volume fractions compared to the reference case. During the following stage (400 s to 1250 s), the increased quantity of liquid PCM results in a more considerable influence of natural convection. Consequently, the cases with higher CuO volume fractions, specifically the 5 wt.%, 7 wt.%, and 9 wt.%, exhibit the lowest mass fraction. This phenomenon is due to the higher density of the NEPCM resulting from the increased volume fraction of nanoparticles, which subsequently diminishes the impact of natural convection. However, in the final stage, the enhanced thermal conductivity compensates for the density increase, leading to the cases with the highest CuO volume fractions exhibiting the greatest liquid fraction and lowest melting times. The complete melting times for the reference case, 1 wt.%, 3 wt.%, 5 wt.%, 7 wt.%, and 9 wt.% are 2768 s, 2687 s, 2559 s, 2383 s, 2284 s, and 2196 s, respectively, indicating the positive impact of increased nanoparticle volume fractions on the regenerator's power density.

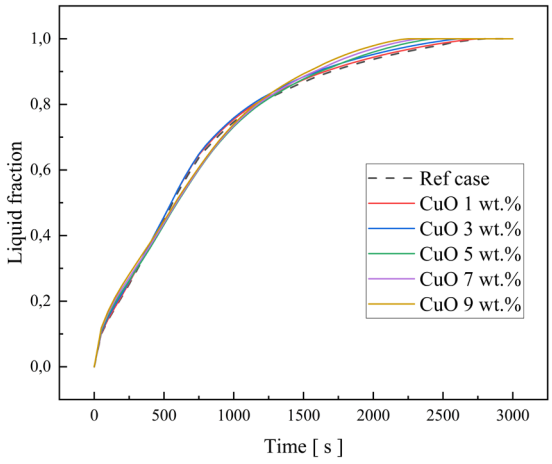

Fig. 3. Effect of nanoparticles volume fraction on the PCM liquid fraction with time.

While the positive impact of nanoparticles on the charging rate of the regenerator is evident, assessing their influence on the stored energy remains critical, as an efficient LTESS is defined by both high energy density and power density. Fig. 4 depicts the temporal progression of stored energy for the different cases. Notably, the reference case achieves the

highest total energy storage at complete melting, amounting to 241.3 KJ/Kg. The addition of CuO nanoparticles results in a reduction in the total stored Energy.

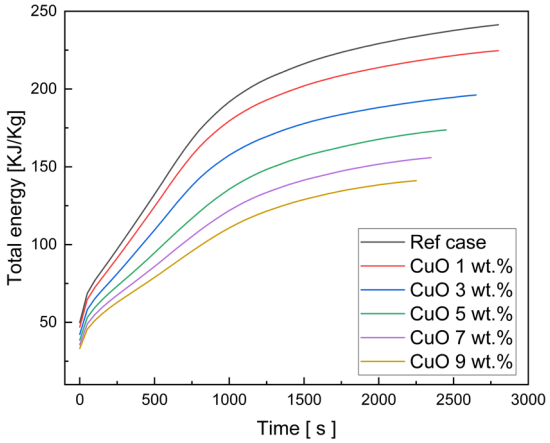

Fig. 4. Total specific energy storage capacity of different volume fractions.

Specifically, cases with 1 wt.%, 3 wt.%, 5 wt.%, 7 wt.%, and 9 wt.% achieve complete melting with corresponding stored energy values of 225 KJ/Kg, 196 KJ/Kg, 174 KJ/Kg, 156 KJ/Kg, and 141 KJ/Kg, respectively. It is noteworthy that the total melting time for cases with 1 wt.%, 3 wt.%, 5 wt.%, 7 wt.%, and 9 wt.% is reduced by 3%, 8%, 14%, 17%, and 21%, respectively, in comparison to the reference case. Correspondingly, the stored energy experiences reductions of 7%, 19%, 28%, 35%, and 42% for the same cases. The results demonstrate that while the addition of CuO nanoparticles enhances the charging rate of the regenerator, it simultaneously leads to a reduction in total stored energy. Balancing these trade-offs is essential in optimizing the performance of the system for practical applications.

3.2 Impact of nanoparticles on various regenerator's configurations

As previously shown, the incorporation of nanoparticles within a case devoid of enhancement techniques, improves power density but also leads to a notable reduction in stored energy. Nevertheless, the behaviour of the system when combined with heat intensification methods like fins and eccentricity remains to be explored. This exploration aims to discern the extent of the benefits of nanoparticles integration when applied to a LTESS with diverse enhancement techniques. Fig 5. Depicts the liquid fraction temporal evolution of different cases: the case with non-uniform fins, eccentricity, and combined fins with eccentricity, with and without 3 wt.% of CuO nanoparticles. As can be seen, the influence of nanoparticle addition is less pronounced in cases employing enhancement techniques compared to the reference case. The total melting time for the finned case, finned case with CuO, eccentric case, eccentric case with CuO, combined case, and combined case with CuO is 1050 s, 1008 s, 1274 s, 1294 s, 1171 s, and 1082 s, respectively. Notably, the finned case shows a 4% improvement with the addition of nanoparticles, the combined case exhibits an 8% enhancement, while the eccentric case surprisingly experiences a 2% decrease. The observed variation among the different cases is attributed to the influence of natural convection and conduction in the melting process.

For instance, in the eccentric case, natural convection plays a significant role compared to other cases. The addition of nanoparticles increases the PCM density, reducing buoyancy forces and impeding heat transfer within the regenerator. Indeed, the increase in thermal conductivity induced by the addition of nanoparticles, proved insufficient to compensate for

the reduction in the natural convection, resulting in an overall increase in the total melting time. In the finned case, the extended surfaces impede the circulation of the PCM, reducing the impact of natural convection. Consequently, the addition of nanoparticles results in improved heat transfer, albeit less significantly compared to the combined case (4% decrease in the finned case versus 8% in the combined case).

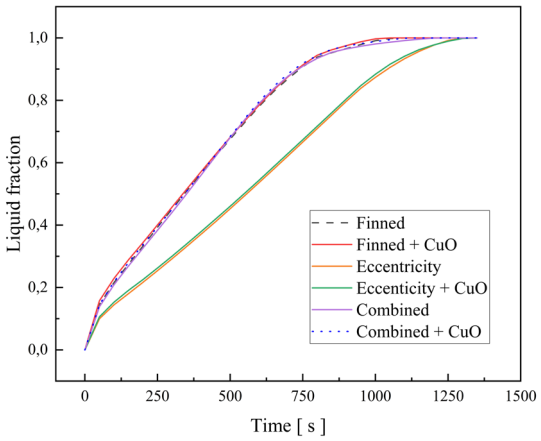

Fig. 5. Temporal evolution of liquid fraction of different enhancement techniques with and without addition of nanoparticles.

To gain further insight into this observation, Fig. 6 illustrates the melting fronts and velocity contours of the different cases. With the less prominent improvement in melting time, the distinction between cases with and without nanoparticles is not readily discernible in the liquid/solid fronts. However, the velocity contours clearly indicate variations in buoyancy forces when nanoparticles are introduced. It is evident, as mentioned earlier, that the eccentric case exhibits the highest influence of natural convection, followed by the finned case, and lastly, the combined case. This justifies the enhancement rates for each case, confirming that the greater the effect of natural convection in the regenerator, the weaker the impact of nanoparticles. The reason for the combined case having the lowest effect of natural convection is the presence of fins in the upper part of the regenerator, which is the section most affected by natural convection, which hinders the liquid PCM movement and thus limits the buoyancy forces effect.

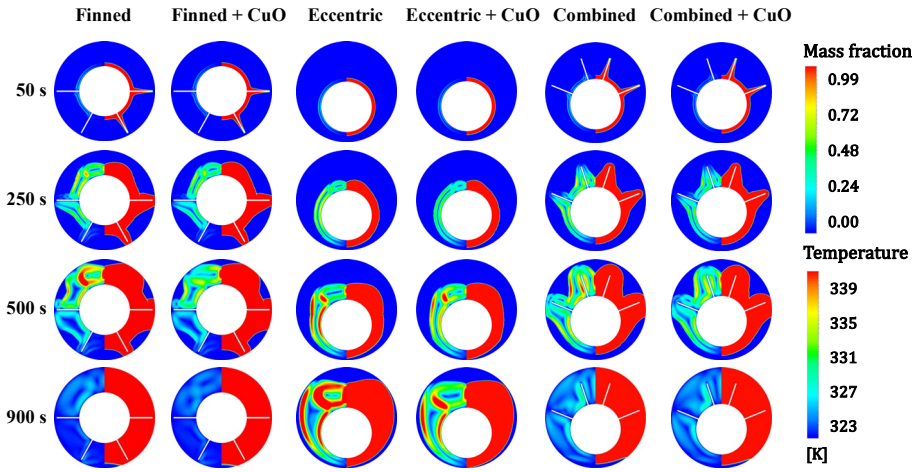

Fig. 6. Contour plots of the melting fronts and velocity of various cases.

4 Conclusion

This study undertook a comprehensive numerical exploration of a horizontal co-axial regenerator employing PCM enhanced with CuO nanoparticles. The primary focus was on assessing the impact of CuO nanoparticles volume fraction on the thermal and energetic performance of the regenerator, followed by examining their influence on total melting time and power densities across different configurations. The following conclusions are drawn:

- CuO nanoparticles enhance the power density of the system, showcasing potential for improved thermal performance.
- The addition of 5% of CuO to the regenerator reduced the melting time and stored energy by 14% and 28%, respectively.
- The addition of nanoparticles reduces the storage capacity of the LTESS, highlighting the need for a balanced consideration of power and energy densities.
- The influence of nanoparticles is less pronounced in cases employing enhancement techniques compared to the reference case.
- The influence of nanoparticles varied based on the regenerator's configuration.
- The finned and combined case show a 4% and 8% reduction in the melting time with the addition of nanoparticles, respectively.
- The eccentric case demonstrates a 2% augmentation in melting time attributed to the increased density of the NEPCM, reducing buoyancy forces and impeding heat transfer within the regenerator.
- the study highlights a significant correlation between the impact of nanoparticles and the natural convection within the regenerator. The greater the influence of natural convection, the weaker the overall impact of nanoparticles on the system.

Acknowledgment

The authors gratefully acknowledge the financial support provided by ENSUS, the Energy Sustainability Chair.

References

[1] M. El Fiti, M. Salihi, Y. Harmen, Y. Chhiti, A. Chebak, F.E. M'Hamdi Alaoui, M. Achak, F. Bentiss, C. Jama, Energetic performance optimization of a coaxial phase change material (PCM) regenerator, J. Energy Storage. 50 (2022) 104571. https://doi.org/10.1016/J.EST.2022.104571.

[2] M.E.H. Amagour, M. Bennajah, A. Rachek, Numerical investigation and experimental validation of the thermal performance enhancement of a compact finned-tube heat exchanger for efficient latent heat thermal energy storage, J. Clean. Prod. 280 (2021) 124238. https://doi.org/10.1016/J.JCLEPRO.2020.124238.

[3] R. Karami, B. Kamkari, Experimental investigation of the effect of perforated fins on thermal performance enhancement of vertical shell and tube latent heat energy storage systems, Energy Convers. Manag. 210 (2020) 112679. https://doi.org/10.1016/j.enconman.2020.112679.

[4] X. Guo, X. Han, J. Lin, S. Liu, Z. Han, Effect of eccentricity and V-shaped fins on the heat transfer performance of a phase change heat storage system, J. Energy Storage. 73 (2023) 108833. https://doi.org/10.1016/j.est.2023.108833.

[5] Y. Xu, Z.J. Zheng, S. Chen, X. Cai, C. Yang, Parameter analysis and fast prediction of the optimum eccentricity for a latent heat thermal energy storage unit with phase

change material enhanced by porous medium, Appl. Therm. Eng. 186 (2021) 116485. https://doi.org/10.1016/j.applthermaleng.2020.116485.

[6] Y. Harmen, Y. Chhiti, M. El Fiti, M. Salihi, C. Jama, Eccentricity analysis of annular multi-tube storage unit with phase change material, J. Energy Storage. 64 (2023) 2352–152. https://doi.org/10.1016/j.est.2023.107211.

[7] M. Alizadeh, K. Hosseinzadeh, M.H. Shahavi, D.D. Ganji, Solidification acceleration in a triplex-tube latent heat thermal energy storage system using V-shaped fin and nano-enhanced phase change material, Appl. Therm. Eng. 163 (2019) 114436. https://doi.org/10.1016/j.applthermaleng.2019.114436.

[8] A.M. Abdulateef, S. Mat, K. Sopian, J. Abdulateef, A.A. Gitan, Experimental and computational study of melting phase-change material in a triplex tube heat exchanger with longitudinal/triangular fins, Sol. Energy. 155 (2017) 142–153. https://doi.org/10.1016/j.solener.2017.06.024.

[9] P. Yan, W. Fan, Y. Yang, H. Ding, A. Arshad, C. Wen, Performance enhancement of phase change materials in triplex-tube latent heat energy storage system using novel fin configurations, Appl. Energy. 327 (2022) 120064. https://doi.org/10.1016/j.apenergy.2022.120064.

[10] N. Bianco, S. Busiello, M. Iasiello, G.M. Mauro, Finned heat sinks with phase change materials and metal foams: Pareto optimization to address cost and operation time, Appl. Therm. Eng. 197 (2021) 117436. https://doi.org/10.1016/J.APPLTHERMALENG.2021.117436.

[11] Y. Shuai, C. Zhang, X. Hu, S. He, X. lu Gong, A comprehensive structural parameter for optimization of thermal performance of PCM embedded in periodic cuboid cell metal foam, Int. Commun. Heat Mass Transf. 146 (2023) 106936. https://doi.org/10.1016/j.icheatmasstransfer.2023.106936.

[12] R.S. Ferfera, B. Madani, Thermal characterization of a heat exchanger equipped with a combined material of phase change material and metallic foams, Int. J. Heat Mass Transf. 148 (2020) 119162. https://doi.org/10.1016/J.IJHEATMASSTRANSFER.2019.119162.

[13] N. Ouahabi, A. Chebak, M. Berquedich, O. Kamach, M. Zegrari, Deploying Digital Twin in Manufacturing Systems: Scope and Requirements, Lect. Notes Networks Syst. 711 LNNS (2023) 639–650. https://doi.org/10.1007/978-3-031-37717-4_41/FIGURES/2.

[14] K. Merlin, D. Delaunay, J. Soto, L. Traonvouez, Heat transfer enhancement in latent heat thermal storage systems: Comparative study of different solutions and thermal contact investigation between the exchanger and the PCM, Appl. Energy. 166 (2016) 107–116. https://doi.org/10.1016/j.apenergy.2016.01.012.

[15] J. Zhang, Z. Cao, S. Huang, X. Huang, K. Liang, Y. Yang, H. Zhang, M. Tian, M. Akrami, C. Wen, Improving the melting performance of phase change materials using novel fins and nanoparticles in tubular energy storage systems, Appl. Energy. 322 (2022) 119416. https://doi.org/10.1016/j.apenergy.2022.119416.

[16] J.M. Mahdi, E.C. Nsofor, Melting enhancement in triplex-tube latent thermal energy storage system using nanoparticles-fins combination, Int. J. Heat Mass Transf. 109 (2017) 417–427. https://doi.org/10.1016/j.ijheatmasstransfer.2017.02.016.

[17] M. Sheikholeslami, Analyzing melting process of paraffin through the heat storage with honeycomb configuration utilizing nanoparticles, J. Energy Storage. 52 (2022) 104954. https://doi.org/10.1016/j.est.2022.104954.

[18] C.P. V.R. Voller, A Fixed grid numerical modelling methodology for convection diffusion mushy region phase change problems, Int. Jounal Heat Mass Transf. 30 (1978) 1709–1719.

[19] R. Qaiser, M.M. Khan, L.A. Khan, M. Irfan, Melting performance enhancement of PCM based thermal energy storage system using multiple tubes and modified shell designs, J. Energy Storage. 33 (2021) 102161. https://doi.org/10.1016/j.est.2020.102161.

[20] M. Parsazadeh, X. Duan, Numerical and statistical study on melting of nanoparticle enhanced phase change material in a shell-and-tube thermal energy storage system, Appl. Therm. Eng. 111 (2017) 950–960. https://doi.org/10.1016/j.applthermaleng.2016.09.133.

[21] M. Nitsas, I.P. Koronaki, Performance analysis of nanoparticles-enhanced PCM: An experimental approach, Therm. Sci. Eng. Prog. 25 (2021) 100963. https://doi.org/10.1016/j.tsep.2021.100963.

[22] N.S. Dhaidan, J.M. Khodadadi, T.A. Al-Hattab, S.M. Al-Mashat, Experimental and numerical investigation of melting of NePCM inside an annular container under a constant heat flux including the effect of eccentricity, Int. J. Heat Mass Transf. 67 (2013) 455–468. https://doi.org/10.1016/j.ijheatmasstransfer.2013.08.002.